1. Ultrasonic adsorption kinetics and adsorption isotherms

The adsorption performance of methylene blue (MB) on several catalysts was systematically evaluated at 25℃using dark adsorption experiments (Fig.1). This study investigated the effects of incorporating bio-carbon (BC), graphite carbon nitride (g-C_3N_4), and zinc oxide (ZnO) on the adsorption performance of the catalyst. The BC/ZnO/g-C_3N_4 composite exhibited the fastest adsorption kinetics, particularly during the initial 10 minutes, indicating an increased availability of active sites and stronger affinity for MB. BC provides a high surface area and porous structure, offering abundant adsorption sites and improving mass transfer. The incorporation of g-C_3N_4 further enhanced adsorption, likely due to its two-dimensional layered morphology and nitrogen-rich composition, which introduce additional adsorption centers and strengthen interactions with MB. Consequently, the BC/ZnO/g-C_3N_4 catalyst was selected for subsequent modification and further study.

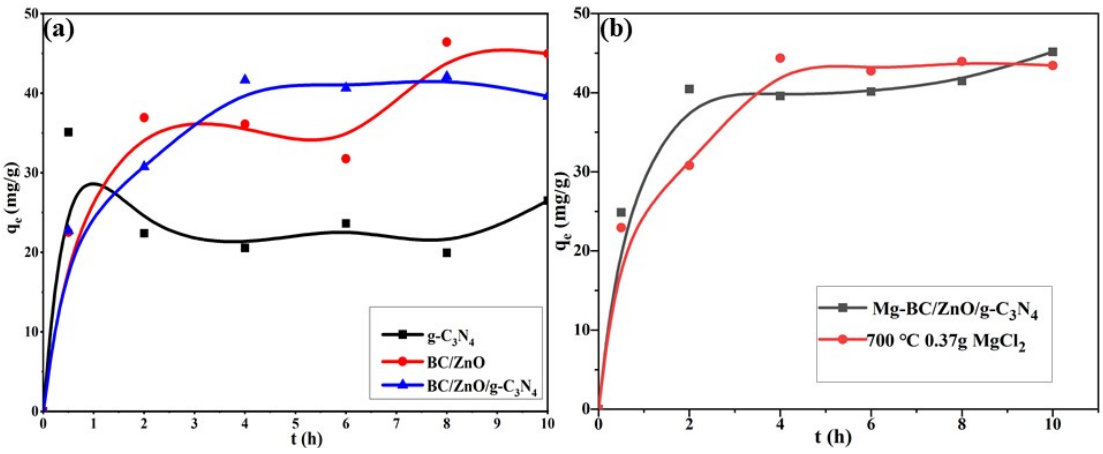

Fig.1 Time-dependent adsorption capacity of MB adsorption onto different catalyst [$V_{[MB]}$ = 40 mL , C_0=30 mg/L，[catalyst] = 0.5 g/L , 25℃]

The catalysts were prepared at different carbonization temperatures to assess the effect on adsorption performance (Fig.1b). Samples carbonized at 550 °C exhibited markedly faster adsorption kinetics, reaching high removal within minutes, whereas samples treated at 700 °C required up to 2 h to achieve comparable removal. These results indicate that maintaining the g-C_3N_4 layered structure at low temperatures (550 °C) promotes adsorption. In contrast, above 600 °C, g-C_3N_4 undergoes decomposition and nitrogen loss, leading to structural collapse and a reduction in available

adsorption sites. These structural changes can modify the catalyst's surface properties and consequently degrade adsorption kinetics. Incorporation of Mg likely modifies the physicochemical characteristics of the catalyst surface, potentially enhancing the number of active sites or altering surface charge to strengthen electrostatic interactions with methylene blue (MB) and enhancing adsorption. However, this beneficial effect is evident only when combined with optimal carbonization parameters.

Adsorption kinetics and thermodynamics were investigated, and the results are summarized in Tables 1 and Table 2. The linear correlation coefficients (R^2) of the pseudo-second-order kinetic model exceeded 0.9 for g-C_3N_4, BC/ZnO/g-C_3N_4, Mg-BC/ZnO/g-C_3N_4, and the samples prepared with 0.37 g $MgCl_2$ and carbonized at 700 °C, indicating that the adsorption kinetics are best described by the pseudo-second-order model. This strongly suggests that the adsorption rate is controlled primarily by chemisorption, which involves electron sharing or exchange between the adsorbent and adsorbate, rather than by simple physisorption. Comparison of adsorption isotherms shows that the Freundlich model provides a better fit than the Langmuir model for all samples, including g-C_3N_4, ZnO/BC, BC/ZnO/g-C_3N_4, Mg-BC/ZnO/g-C_3N_4, and 0.37 g $MgCl_2$ at 700 °C. This outcome indicates surface heterogeneity and multilayer adsorption and implies nonuniform affinities of adsorbate molecules for different active sites on the adsorbent/catalyst surface.

Table 1 Parameters of kinetics for the adsorption of MB (25℃)

	Pseudo-first-order model			Pseudo-second-order model		
	q_e (mg/g)	K_1	R^2	q_e (mg/g)	K_2	R^2
g-C_3N_4	23.6361	-0.0368	0.0199	35.1159	0.0415	0.9324
ZnO/BC	36.1155	-0.2444	0.6740	46.4166	0.0212	0.0212
BC/ZnO/g-C_3N_4	41.6781	-0.2731	0.0221	42.0902	0.0234	0.9911
Mg-BC/ZnO/g-C_3N_4	39.5809	-0.1680	0.8377	45.1607	0.0220	0.9919
700 ℃ 0.37g $MgCl_2$	44.3564	-0.403	0.7811	44.3564	0.0214	0.9928

Table 2 Parameters of isotherm for the adsorption of MB (25℃)

	Langmuir isotherm			Freundlich isotherm	
	k	R^2	1/n	k_f	R^2
g-C_3N_4	0.2680	1	1	3.7315	1
ZnO/BC	0.2024	0.7682	0.7885	6.2660	0.8262
BC/ZnO/g-C_3N_4	0.2667	1	1	3.7502	1
Mg-BC/ZnO/g-C_3N_4	0.2650	0.9986	1	3.7315	1
700 ℃ 0.37g $MgCl_2$	0.2371	0.7175	0.2371	0.1274	0.6552

Kinetic and isotherm analyses indicate that adsorption is a complex, chemically driven process occurring on a heterogeneous surface characterized by a distribution of binding energies. This finding is consistent with the catalyst's composite structure, in which BC, ZnO, g-C_3N_4, and Mg species provide distinct active sites and interaction modes.

2.Catalytic performance

The effects of catalyst dosage (Fig.2a), H_2O_2 dosage (Fig.3a), pH (Fig.3c), and initial methylene blue (MB) concentration (Fig.3e) on degradation performance were investigated. Increasing the catalyst dosage from 0.3 to 0.7 g/L enhanced MB degradation, with a rapid improvement up to 0.5 g/L followed by a plateau between 0.5 and 0.7 g/L, indicating an optimal loading beyond which further additions yield no significant enhancement. At low catalyst loadings, the limited number of active sites restricts H_2O_2 activation and the generation of reactive oxygen species (ROS), thereby reducing degradation efficiency. As the dosage increases, the greater availability of active sites accelerates degradation. However, above approximately 0.5 g/L the rate plateaus, likely owing to site saturation of active sites, mass-transfer limitations, catalyst agglomeration that reduces accessible surface area, and impaired light penetration or reactant diffusion.

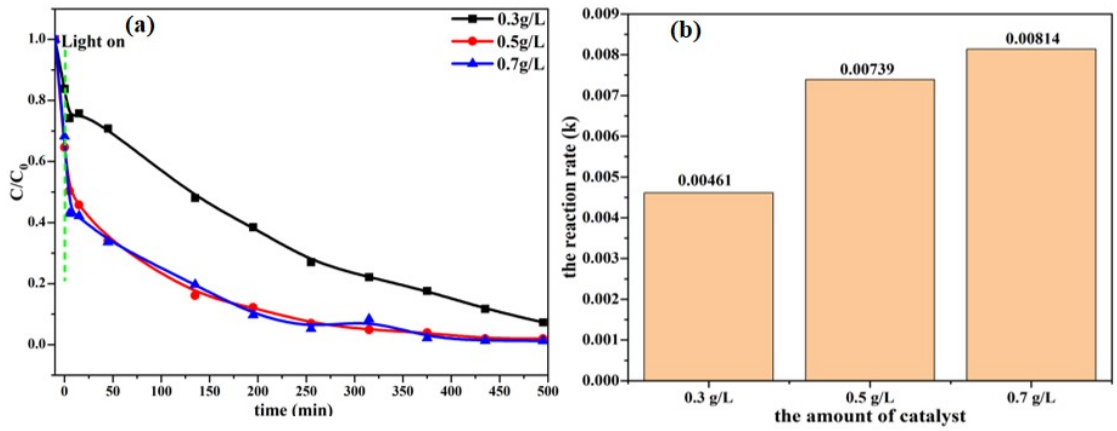

Fig.2 (a) The effect of the amount of catalyst; (b) its catalytic degradation rates

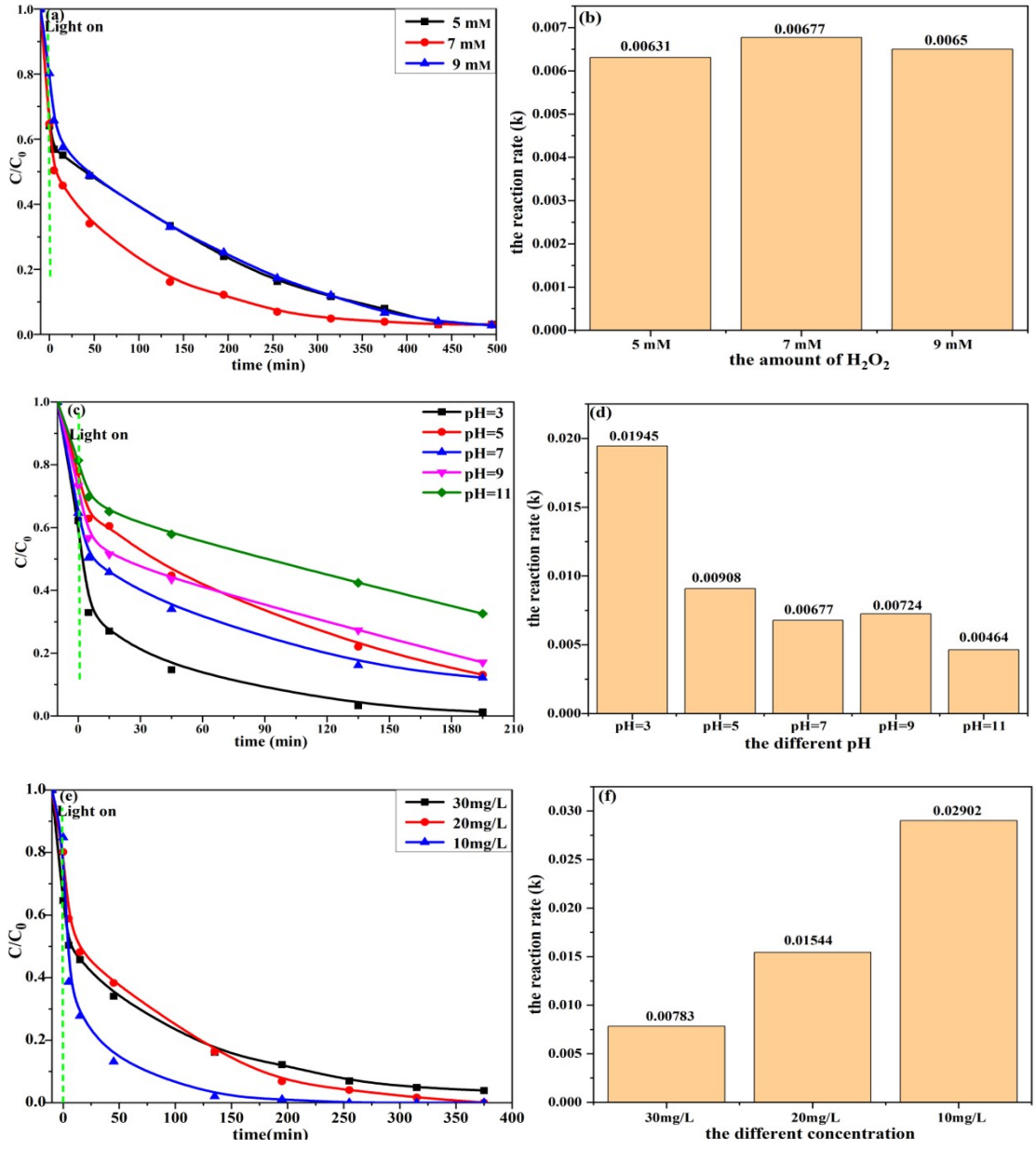

Fig.3 (a) The effect of the amount of H_2O_2 (b) and its catalytic degradation rates; (c) the effect of the pH (d) and its catalytic degradation rates; (e) the effect of the MB

concentration (f) and its catalytic degradation rates

The MB degradation rate increased with H_2O_2 concentration up to an optimum at 7 mM, and declined at higher concentrations. This indicates that 7 mM H_2O_2 maximizes production of hydroxyl radicals (•OH) responsible for degradation. At lower H_2O_2 levels, the availability of oxidizing•OH radicals rises with increasing H_2O_2, enhancing degradation. However, concentrations above 7 mM result in excess H_2O_2 that scavenges hydroxyl radicals (•OH) via side reactions, thereby reducing degradation efficiency.

The catalyst demonstrated enhanced MB degradation under acidic conditions, achieving maximum efficiency at pH=3. At acidic pH, hydrogen-bonding interactions between the catalyst surface and MB are strengthened, increasing MB adsorption. Enhanced adsorption promotes more effective activation of H_2O_2 and subsequent generation of reactive species, thereby accelerating degradation[1, 2]. Under alkaline conditions, a decrease in catalytic activity may be attributed to weakened adsorption due to reduced hydrogen bonding, or possible catalyst surface charge alterations that repel the negatively charged dye molecules or intermediates. In addition, the stability of hydroxyl radicals (•OH) and the dominant H_2O_2 decomposition pathways are pH-dependent, which further reduces degradation rates.

With H_2O_2 fixed at 7 mM and catalyst loading at 0.5 g/L, the effect of initial MB concentration on degradation efficiency was examined. After 195 min, removal efficiencies were 99%, 93%, and 88% for initial MB concentrations of 10 mg/L, 20 mg/L, and 30 mg/L, respectively. These results show that the catalyst effectively degrades low MB concentrations in a short time. However, as the initial concentration increases, the availability of active sites and reactive species per dye molecule decreases, and intensified competition for adsorption sites reduces the degradation rate.

3.The design of the purification cup

Outdoor water purifiers were first introduced in Europe and North America, established products include BeFree, Katadyn Hiker Pro, Katadyn Vario, and the

Katadyn Combi Filter. Table 3 summarizes the key parameters, functions, and typical applications of these devices. A detailed analysis of Table 3 reveals common limitations of current market offerings, notably inadequate removal of organic contaminants and limited filtration capacity. To address these shortcomings and better meet the needs of outdoor users, we developed a novel purification cup that combines improved filtration technology with a user-friendly, portable design. The device structure and functional features are shown in Figs. 4 and 5.

Table 3 The comparison of purification cup parameters

Trademark					
Parameter	model	Befree	Katadyn Hiker Pro	Katadyn Vario	Katadye Combi Filter
	weight	58 g	310 g	460 g	580 g
	quality time	2 years	2 years	2 years	2 years
	Purified water capacity	1000 L	1150 L	2000 L	50000 L
	purification technics	Fiberglass	Fiberglass	fiberglass activated carbon ceramic wafer	activated carbon cartidge ceramic fiber Ceramic element
Function	Effective against protozoa	√	√	√	√cartidge
	Effectively combat bacteria	√	√	√	√
	Effectively combat viruses	√	√	√	√
	Can filter out particles	√	√	√	√
	Can filter out organic substances	╳	╳	╳	╳
Application	Clear surface water	√	√	√	√
	Slightly turbid water	√	√	√	√
	Turbid water	√	√	√	√
	Improve the smell	√	√	√	√
	tap water	√	√	√	√

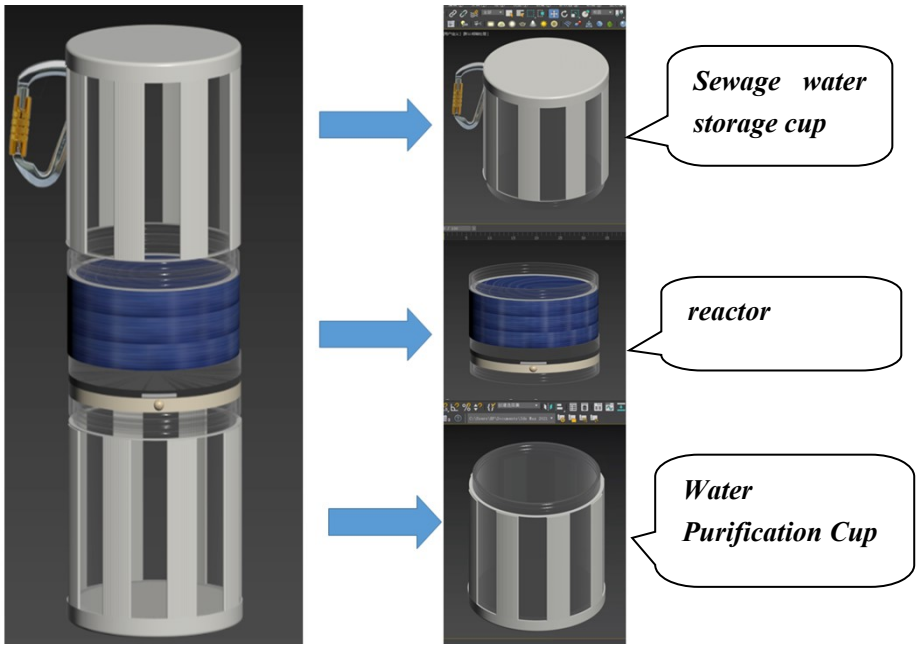

Fig.4 The appearance diagram of Purification cup

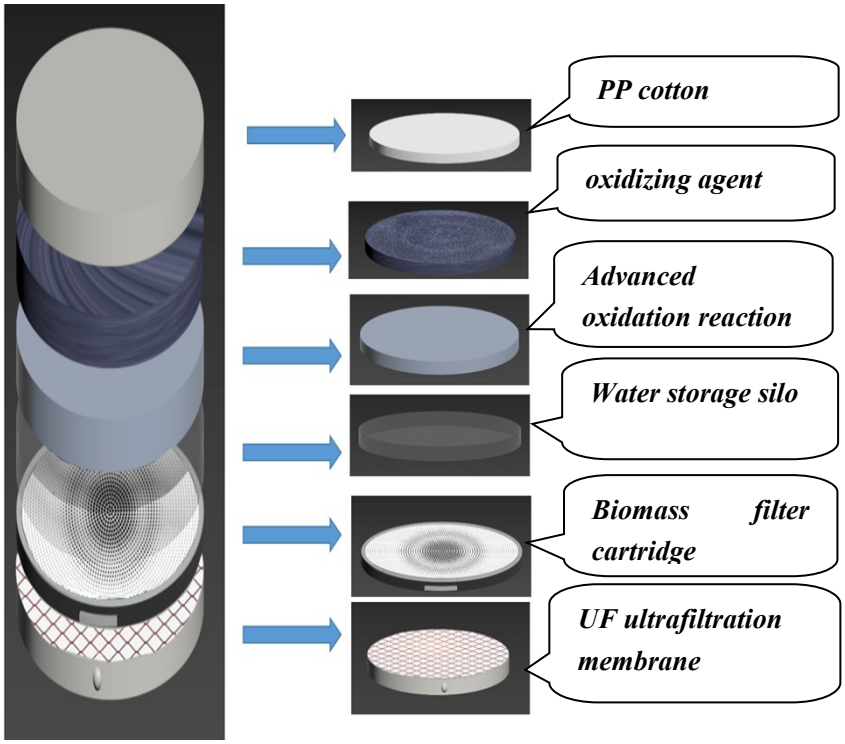

Fig.5 The Diagram of the reactor internal composition

3.1 Product Description

The device is an outdoor water purifier that integrates advanced oxidation processes (AOPs), filtration, and adsorption. Its internal components include a polypropylene (PP) cotton prefilter, an AOP reactor containing a heterogeneous

catalyst, a biomass-based filter element, and an ultrafiltration (UF) membrane. TThe catalyst facilitates the oxidation of organic contaminants to CO_2 and H_2O. The biomass filter is produced in situ from the natural polysaccharides sodium alginate (SA) and carboxymethyl cellulose (CMC), which are cross-linked to form a matrix that immobilizes the catalyst and enhances adsorption and biodegradation[3]. The abundant hydroxyl and carboxyl functional groups of SA and CMC facilitate chelation and adsorption of metal ions, improving ion removal to levels consistent with drinking-water standards. The synergistic action of the advanced oxidation process and the biomass-based adsorbent module yields treated water that complies with potable-water regulations. Consequently, the system ensures safe, potable water and provides a reliable, user-friendly solution suitable for portable and outdoor water purification applications.

PP cotton and UF filtration membranes are commercially available. The catalyst can be synthesized by a straightforward procedure, and the biomass adsorbent is prepared in the laboratory. The biomass adsorbent is a simple, well-established, and effective method for metal-ion removal and offers advantages in storage and handling. The UF membrane used is a microbial ultrafiltration membrane that efficiently removes bacteria and other microorganisms from water.

Supplementary Table 4. The formula for calculating the elemental content in the catalyst.

The elemental content of the sample is Cx	Element content W (%) of the sample
$C_x(\mathrm{mg/kg}) = \frac{C_0(mg/L) * f * V_0(mL) * 10^{-3}}{m(g) * 10^{-3}} = \frac{C_1(mg/L) * V_0(mL)}{m(g) * 10^{-3}}$	$W(\%) = \frac{C(mg/kg)}{10^6} * 100\%$
m_0: Sample mass m_0 (g); **V_0:** Constant volume (mL);	
C_0: Test the elemental concentration of the solution (mg/L); **f:** Dilution factor; **C_1:** The elemental concentration of the original sample digestion solution	**C:** The elemental content of the sample is Cx

(mg/L);

Supplementary Table 5. The elemental content of $Zn^{2+}$and Mg^{2+} ions in the catalyst.

entry	m_0 (g)	V_0 (mL)	The elemental	C_o (mg/L)	f	C_1 (mg/L)	C_x (mg/kg)	W (%)	average
1	0.0537	25	Mg	3.3259	1	3.3259	1548.3787	0.1548%	
1	0.0537	25	Mg	3.3607	1	3.3607	1564.5500	0.1565%	0.1566%
1	0.0537	25	Mg	3.4061	1	3.4061	1585.6998	0.1586%	
2	0.0537	25	Zn	1.1676	1000	1167.6416	543594.7812	54.3595%	
2	0.0537	25	Zn	1.1661	1000	1166.0668	542861.6341	54.2862%	54.2594%
2	0.0537	25	Zn	1.1634	1000	1163.4131	541626.2151	54.1626%	

Supplementary : The chemical reaction equation for the preparation of the catalyst.

$$CH_4N_2S + H_2O \longrightarrow CO(NH_2)_2 + H_2S$$

$$CO(NH_2)_2 + 3H_2O \longrightarrow CO_2 + 2NH_3{\cdot}H_2O$$

$$Zn^{2+} + 2NH_3{\cdot}H_2O \longrightarrow Zn(OH)_2\downarrow + 2NH_4^+$$

$$Zn(OH)_2 \xrightarrow{\triangle} ZnO\ (s) + H_2O\uparrow$$

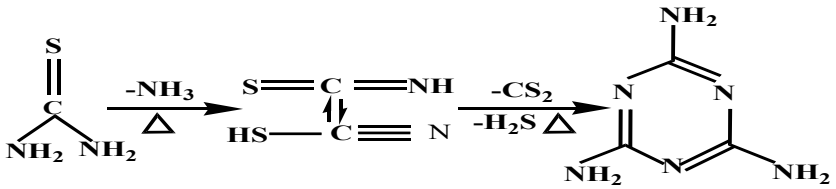

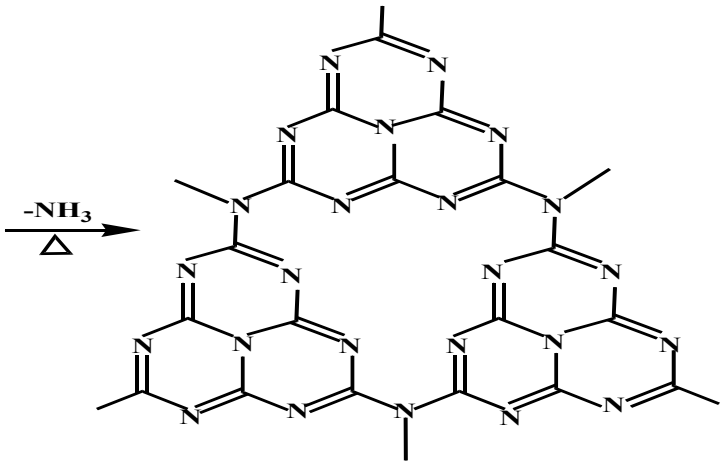

Supplementary Table 6. The yield of the catalyst.

entry	catalyst	Weight of the sample before carbonization	carbonization temperature	yield (g)
1	g-C_3N_4	2.6067	550℃	0.2053
2	BC-Zn	3.1247	550℃	1.5562
3	BC/ZnO/g-C_3N_4	3.7852	550℃	1.0985
4	Mg-BC/ZnO/g-C_3N_4	3.8614	550℃	1.0882
5	700 °C 0.23g $MgCl_2$	3.8351	700℃	0.6624

Supplementary Table7. The amount of metal ion dissolution from the catalyst into the reaction solution

ion mg/L	Number of cycle 1	Number of cycle 2	Number of cycle 3
Zn^{2+}	4.726	3.163	1.381
Mg^{2+}	3.590	2.758	2.821

At the end of the reaction, ICP-OES was used to determine the amount of metal ions leached from the catalyst into the reaction solution shown in **Table S7**. After 3 cycles of recycle experiments, the leaching rates of zinc ion and Magnesium ion were accorded with the discharge level in water (Zn^{2+}_{max} = 5 mg/L).

References:

1. Bajiri, M.A., Hezam, A., Namratha, K., Viswanath, R., Drmosh, Q.A., Bhojya Naik, H.S., Byrappa, K., CuO/ZnO/g-C_3N_4 heterostructures as efficient visible light-driven photocatalysts. Journal of Environmental Chemical Engineering 2019, 7(5), 103412.
2. Li, C., Xiong, Z., Zhang, J., Wu, C., The Strengthening Role of the Amino Group in Metal-Organic Framework MIL-53 (Al) for Methylene Blue and Malachite Green Dye Adsorption. Journal of Chemical & Engineering Data 2015, 60(11), 3414-3422.
3. Zheng, Y., Sun, K., Wen, N., Rao, H., Ye, H., Yang, B., An all-biomass adsorbent: competitive removal and correlative mechanism of Cu^{2+}, Pb^{2+}, Cd^{2+} from multi-element aqueous solutions. Polymer Bulletin 2023, 80(12), 12619-12640.